

RSC Advances



This is an *Accepted Manuscript*, which has been through the Royal Society of Chemistry peer review process and has been accepted for publication.

Accepted Manuscripts are published online shortly after acceptance, before technical editing, formatting and proof reading. Using this free service, authors can make their results available to the community, in citable form, before we publish the edited article. This *Accepted Manuscript* will be replaced by the edited, formatted and paginated article as soon as this is available.

You can find more information about *Accepted Manuscripts* in the [Information for Authors](#).

Please note that technical editing may introduce minor changes to the text and/or graphics, which may alter content. The journal's standard [Terms & Conditions](#) and the [Ethical guidelines](#) still apply. In no event shall the Royal Society of Chemistry be held responsible for any errors or omissions in this *Accepted Manuscript* or any consequences arising from the use of any information it contains.

Fabrication of Tunable Au SERS Nanostructures by a Versatile Technique and Application in Detecting Sodium Cyclamate

Jing Chen^{1,2}, Wen Shen², Biswajit Das^{2,*}, Yiyan Li³, Gaowu Qin^{1,*}

1. Key Laboratory for Anisotropy and Texture of Materials (Ministry of Education), Northeastern University, Shenyang 110819, China

2. Nevada Nanotechnology Center, Howard R. Hughes College of Engineering, University of Nevada, Las Vegas, NV 89154-4026, USA

3. Department of Electrical and Computer Engineering, University of Nevada, Las Vegas, NV 89154, USA

*Corresponding author. dasb@unlv.nevada.edu (B. Das), qingw@smm.neu.edu.cn (G. W. Qin).

Abstract

In this work, three typical morphologies of SERS substrates, which composed of Au nanoparticles, short Au nanowires (NWs) with small Au nanoparticles filled in the nanogaps and long Au NWs intertwining each other into a self-supporting film, were fabricated by a versatile nanocluster fabrication technique, respectively. This physical technique is easy to implement, cost-effective, and the fabricated SERS substrate is large-area, owns good homogeneity and long-term stability. More importantly, the SERS substrates made by this physical method will not incorporate the reductants and surfactant chemicals, thus can yield clean surfaces, which is suitable for analytes with weak affinity to substrate surface. Then the fabricated substrate with the highest enhancement factor (EF) successfully acquired the SERS spectrum of sodium cyclamate, a restricted food additive, with good signal-noise-ratio. Finally, a set of piecewise-linear equations was provided according to the correlation between SERS intensity and sodium cyclamate concentration, with a detection limit down to 1.6×10^{-9} M.

Keywords

gold nanoparticle; gold nanowire; physical vapor deposition; sodium cyclamate; surface-enhanced Raman spectroscopy

1. Introduction

Since its first discovery, surface-enhanced Raman spectroscopy (SERS) has attracted great attentions due to its marvelous enhancement.^[1,2] As SERS can provide an insight into the sharp and distinguishable vibrational structure of molecules, together with its ultrasensitive and nondestructive detection property, make SERS an ideal approach for the detection of biological molecules and chemical molecules.^[3-18] Fabrication of reliable and high enhanced SERS substrates is the necessary prerequisite for efficient SERS detection.

SERS substrates composed of nanoparticle, nanowire (NW) and nanofilm arrays are three typical SERS substrate patterns and have attracted great attentions in the past decades.^[19-25] Chemical synthesis has prevailed in producing nanoparticles and NWs. The strategies such as self-assembly of nanoparticles into ordered nanoparticle arrays, and assembly of NWs into ordered thin films are popular procedures for organizing the chemical produced nanoparticles and NWs into three typical SERS substrate patterns.^[26-31] Wang *et al.*^[32] described by drying

a 10 μL droplet of cetyltrimethylammonium bromide (CTAB)-capped Au colloid solution on indium-doped tin oxide (ITO) glass resulted in the formation of highly ordered Au spherical nanoparticle arrays with sub-10-nm interparticle spacings. The as-prepared nanoparticle arrays display enormous near-field enhancement at the metallic junctions, and also exhibit high SERS activity, stability, and reproducibility. Tao *et al.*^[33] employed Langmuir-Blodgett (LB) technique to assemble aligned monolayers of silver NWs that are ~ 50 nm in diameter and 2-3 μm in length, with area over 20 cm^2 . The silver NWs were produced using poly(vinyl pyrrolidone) (PVP) as the capping agent. These monolayers of aligned Ag NWs can be readily transferred to any substrates, and exhibit excellent SERS performances in ultrasensitive detection and molecule-specific sensing. More recently, Chen and co-workers^[34] reported an oil-water (two-phase) interfacial self-assembly process for fabricating aligned Ag NW films on solid substrates, which do not need extra pretreatment of either the surface of Ag NWs or the solid substrate. The resultant Ag NW film exhibited highly sensitive and reproducible SERS performance, and As(v) has been detected with single digit ppb sensitivity from actual arsenic-contaminated groundwater samples by using this SERS substrate. Freer and co-workers^[35] demonstrated by using dielectrophoretic assembly method single nanowires have been assembled on electrodes and a 98.5% single nanowire yield have been attained on > 16,000 electrode sites over an area of 400 mm^2 . The balancing of surface, hydrodynamic and dielectrophoretic forces makes the self-assembly process controllable, and the self-limiting process makes low defect assembly possible. The controllability, low defects, together with the ability to position NWs precisely on a substrate, make dielectrophoretic assembly a promising approach for fabricating high-quality SERS substrates.

The techniques used in the above listed literatures are ingenious, and the SERS substrates they fabricated own high enhancement and good reproducibility. However, it is worth noting that when it comes to the chemical syntheses of nanoparticles and NWs, cumbersome procedures will be needed to control nanoparticle sizes and shapes, and also the aspect ratios of NWs. Moreover, the assembly of nanoparticles and NWs also need extra delicate techniques. In Zhang's work,^[36] polyvinylpyrrolidone (PVP) and ascorbic acid were added into purified silver colloid solutions, and well-separated triangular silver nanoplates (SNPs) were produced. Then by immersing the substrates with hydrophobic surfaces into the SNP solution for about 20 h, single-layer self-assembled SNP films can be obtained. More importantly, the nanoparticles and NWs produced by the chemical approaches will inevitably incorporate the reductants and surfactant chemicals, which are hard to remove and will interfere with the SERS detection.^[37-39] In our previous work, by controlling the pH values of alkaline glucose solution, three different Ag SERS substrates composed of monodisperse nanoparticles, nanoparticle-linked NWs, and NW-weaved mesoporous membrane were fabricated, respectively.^[40] Although the SERS substrates produced by the chemical method in our previous work^[40] have a relative high enhancement factor (EF), which can achieve the microorganism identification at the single cell level. However, the substrate interference has to be subtracted from the SERS spectrum obtained from the analyte as the chemical interference, which is not convenient for fast detection.

Herein, employing the physical method to fabricated three typical SERS substrates composed of nanoparticle, NW and nanofilm arrays has been proposed in this work. The physical fabrication technique will yield clean surfaces, thus is suitable for analytes with

weak affinity to substrate surface. What's more, the SERS spectra acquired from these clean substrates are reliable, which is crucial for SERS detection. Considering Ag nanoparticles are not stable under ambient conditions, since they oxidize easily, Au SERS substrates were produced in this work. Nowadays, most of the physical methods for producing nanoparticles have the obstacles in terms of nanoparticle size, material, location, and choice of substrate.^[41] Here, a versatile nanofabrication technique was applied, which can deposit nanoparticles of any material, and can control with nanoparticle size distribution by applying Quadruple mass filter (QMF) on any kind of substrate.^[41] The technique used in this work (deposition of nanoparticles on the uncovered substrates directly) has a higher throughput and lower cost compared to the notable lithography technique, make this direct nanoparticle deposition technique is suitable for scaled-up fabrication of SERS substrates.^[42] Also, only by changing the instrumental parameters, three typical morphologies of SERS substrates (Au nanoparticles, short Au NWs with small Au nanoparticles filled in the nanogaps, and Au NW-weaved, self-supporting films) were fabricated, respectively, which is simple and time-efficient.

Next, to evaluate the performance of SERS substrate, sodium cyclamate was selected as the analyte. Sodium cyclamate is an artificial sweetener, which is used as an additive, and is added to a variety of food, drinks, cosmetics, and medicines. Once ingested, cyclamate is converted to a metabolite, cyclohexylamine, which is harmful and can cause male reproductive effects according to a series of experiments with rats and dogs.^[43-47] The acceptable daily intake for cyclamate has been set at 11 mg/kg by the Joint Expert Committee on Food Additives (JECFA) and at 7 mg/kg by the Scientific Committee on Food of the European Commission (SCFEC) (2000).^[48]

The homogeneity and long-term stability of the SERS substrates were testified, and their EFs were also calculated. By applying the SERS substrate with the highest EF, the SERS spectrum of 0.1 M of sodium cyclamate was successfully acquired, and its SERS intensity is 10 times higher than the SERS intensity obtained from the dense Au film substrate prepared by a common physical fabrication method. The assessment of the concentration dependence was provided at last. This technique is easy to implement, and only by adjusting parameters, three typical Au SERS substrates with clean surfaces can be fabricated, which is suitable for scaled-up fabrication and fast detection.

2. Experimental Section

2.1 Chemicals and Materials

Rhodamine 6G (R6G) ($\geq 95.0\%$, analytical standard), sodium cyclamate (neat, analytical standard), ethanol (analytical standard) were purchased from Sigma-Aldrich, and they were used directly without further purification. Gold target (2.00" Dia. x 0.125" Thick, 99.99%) was purchased from Kurt J. Lesker Company (CA, USA). Silicon wafers were purchased from Silicon Valley Microelectronics (SVM, CA, USA). Ultrapure water ($18.2 \text{ M}\Omega \cdot \text{cm}$) was used for preparation and dilution of R6G solution and sodium cyclamate solution.

2.2 Au SERS substrates fabrication technique

Here we used a nanocluster deposition system (NanoSys 2, Oxford Applied Research Inc.), which incorporates three parts: Nanocluster source, QMF and the main deposition chamber. (1) The schematic of the nanocluster source is shown in Figure 1a. The nanocluster

source consists of a DC magnetron discharge to produce nanoparticles, an aggregation region between the magnetron and the aperture to let the nanoparticles form nanoclusters, and an aperture through which the nanoclusters can go into the QMF. There are several parameters can be adjusted to vary the nanocluster size, such as the power supplied to the magnetron, the rate of the aggregation gases flow, the aperture size, and the distance between the magnetron and the aperture (variable using a linear drive).^[49] The sputtering power was set as 115 W for fabricating all the SERS substrates in this work, which was a moderate value for this system and could generate appropriate sputtering rate. (2) QMF is positioned at the exit of the nanocluster source to measure and select the cluster mass produced by the source. QMF consists of four rods. A voltage with a dc and ac component is applied to one pair, and the negative voltage is applied to the other pair. The nanoclusters produced by the source with various sizes enter into the QMF and move along the axis of the rods. The nanocluster ions are selected according to their mass to charge (m/e) ratio, and ionized clusters with different m/e ratios follow different trajectories because of the quadrupole electric field, so that only ions with certain mass can be transmitted to the ion detector plate and thus fulfill the nanocluster size filtration.^[41,49] There are several parameters which can influence the nanocluster size to pass through are the dc component U , the ac component V , and the frequency. The ratio U/V , called resolution, determines the width of the nanocluster mass band transmitted through the filter. (3) The main deposition chamber, in which the substrate is mounted. Silicon wafer treated with piranha solution (concentrated H_2SO_4 : 30% H_2O_2 = 3:1 volume ratio. *Caution: Piranha solution is extremely corrosive*) was used as the substrate in this work.

A dense gold film was also produced by employing a common physical fabrication technique (sputter coating, 40 mA, 150 s) as control substrate.

All the above substrates were stored separately in commercial aluminum foil for preventing from getting contaminated, and kept in the dark at room temperature prior to use. The commercial aluminum foil was rinsed with ethanol and ultrapure water in advance for degreasing.

2.3 Substrate Homogeneity and Enhancement Capability Measurement

10 μ L of 10^{-4} M of R6G solution was dripped onto the three different Au SERS substrates, respectively. The SERS spectra were acquired immediately after the substrates were dried under ambient conditions. Normal Raman spectrum of 10^{-2} M of R6G solution was also acquired.

2.4 Long-term Stability Measurement of SERS Substrates

After 110 days, three Au SERS substrates were took out carefully from the commercial aluminum foil to test their SERS performance. R6G was employed as the probe molecules, and 10 μ L of 10^{-4} M of R6G solution was dripped onto each Au SERS substrate, respectively.

2.5 Preparation of sodium cyclamate solution

The initial concentration of sodium cyclamate was set as 10^{-1} M and serially diluted down to 10^{-9} M.

2.6 Characterization

The morphologies of the Au SERS substrates were observed by JEOL 7500F field emission scanning electron microscopy (FE-SEM). All SERS and bulk spectra were obtained

using a confocal Horiba Jobin Yvon LabRAM HR Raman spectrometer equipped with a 785 nm laser and a 100× objective to focus the laser onto the sample surface and to collect the scattered light from samples. The incident laser power was attenuated to 0.8 mW or 8 mW for the SERS detection, and the laser power for the normal Raman spectra acquisition of 10^{-2} M bulk R6G solution was set as 80 mW. The frequency of the Raman instrument was calibrated by referring to a silicon wafer at the vibrational band of 520 cm^{-1} . All the measurements were carried out under ambient conditions.

3. Results and Discussion

3.1 Fabrication and characterization of three kinds of Au SERS substrates and clarification of the forming mechanism

3.1.1 Au nanoparticles

First, we turned on the QMF, set a series of parameters to let the nanoparticle size around 10 nm can pass through and get to the silicon wafer substrate. The sputtering power is 115 W. The flow rate of one aggregation gas Ar is 100 standard-state cubic centimeter per minute (sccm), and the other aggregation gas He is 30 sccm. These two aggregation gases can cool and sweep the Au atoms and nanoclusters from the aggregation region to the aperture. The distance between the magnetron and the aperture is set at 50 mm, and the deposition time is 90 s. The FE-SEM image of the Au SERS substrate we got under these parameters is shown in Figure 1b.

Figure 1b shows that the Au SERS substrate fabricated under the above parameters is composed of Au nanoparticles with a mean grain size of about 9-11 nm. The nanoparticles are of high density with very close distance to each other, which is a good pattern for the Raman enhancement since the extremely intense electromagnetic fields are expected at the sites of directly adjacent metallic nanostructures and not from single isolated metallic nanostructures. Because the QMF is on, only the nanoparticle size around 10 nm can pass through the aperture and get to the Si substrate.

3.1.2 Au NW-Au nanoparticle conjugations

Then, we turned off the QMF. The sputtering power is 115 W. The flow rate of one aggregation gas Ar is 100 sccm, and the other aggregation gas He is 30 sccm. The distance between the magnetron and the aperture is set at 50 mm, and the deposition time is 90 s. The FE-SEM image of the Au SERS substrate we got under these parameters is shown in Figure 1c.

Figure 1c shows that the Au SERS substrate is composed of short Au NWs, with some small Au nanoparticles filled in the nanogaps which formed by the NWs connecting to each other. The generated Au nanoparticles move along the aggregation region, while colliding and connecting to each other, thus Au NWs are formed in the nanocluster source. Because the QMF was turned off, the NanoSys 2 does not have any further function of filtration and selection of nanocluster size, which means the Au nanocluster with any size, can pass through the aperture and get to the Si substrate.

To further verify and have a better clarification of this SERS substrate morphology, we shortened the deposition time ($t = 30$ s), and other parameters were kept the same. The corresponding FE-SEM image is shown in Figure 1d. When the deposition time becomes shorter, the silicon wafer substrate only has one layer of Au nanoclusters, which gives a better

view. We can clearly see that the SERS substrate fabricated under these parameters is composed of short Au NWs (the aspect ratio is about 30~100 nanometers long and 20 nanometers wide) and with small Au nanoparticles (the mean grain size is about 9 nm) distributed around the NWs. With the deposition time becomes longer, these short Au NWs will intertwine each other and form nanoporous film with small Au nanoparticles filled in the nanogaps, which is an ideal model for the SERS enhancement.

3.1.3 Au nanofilm

Next, we changed the parameters and got another kind of SERS substrate. Still we turned off the QMF. The sputtering power is 115 W. The flow rate of one aggregation gas Ar is 100 sccm, and the other aggregation gas He is 0 sccm. The distance between the magnetron and the aperture is set at 50 mm, and the deposition time is 90 s (Figure 1e) and 30 s (Figure 1f).

The SERS substrate in Figure 1e is composed of long Au NWs. The NWs intertwine each other randomly into a self-supporting, continuous Au nanofilm. Because the flow rate of one carrier gas He is low to 0 sccm, the time of the generated Au nanoparticles spend in the aggregation region becomes longer,^[50] and the probability of Au nanoparticles collide to each other will increase, thus the longer Au NWs are formed. In contrast, when the deposition time is 30 s (Figure 1f), we can have a better view that the SERS substrate is almost completely composed of long Au NWs, which demonstrates the NW growth strongly depends on the collision probability of the nanoparticles, and this collision probability can be increased by lowering the flow rate of the carrier gas.^[51]

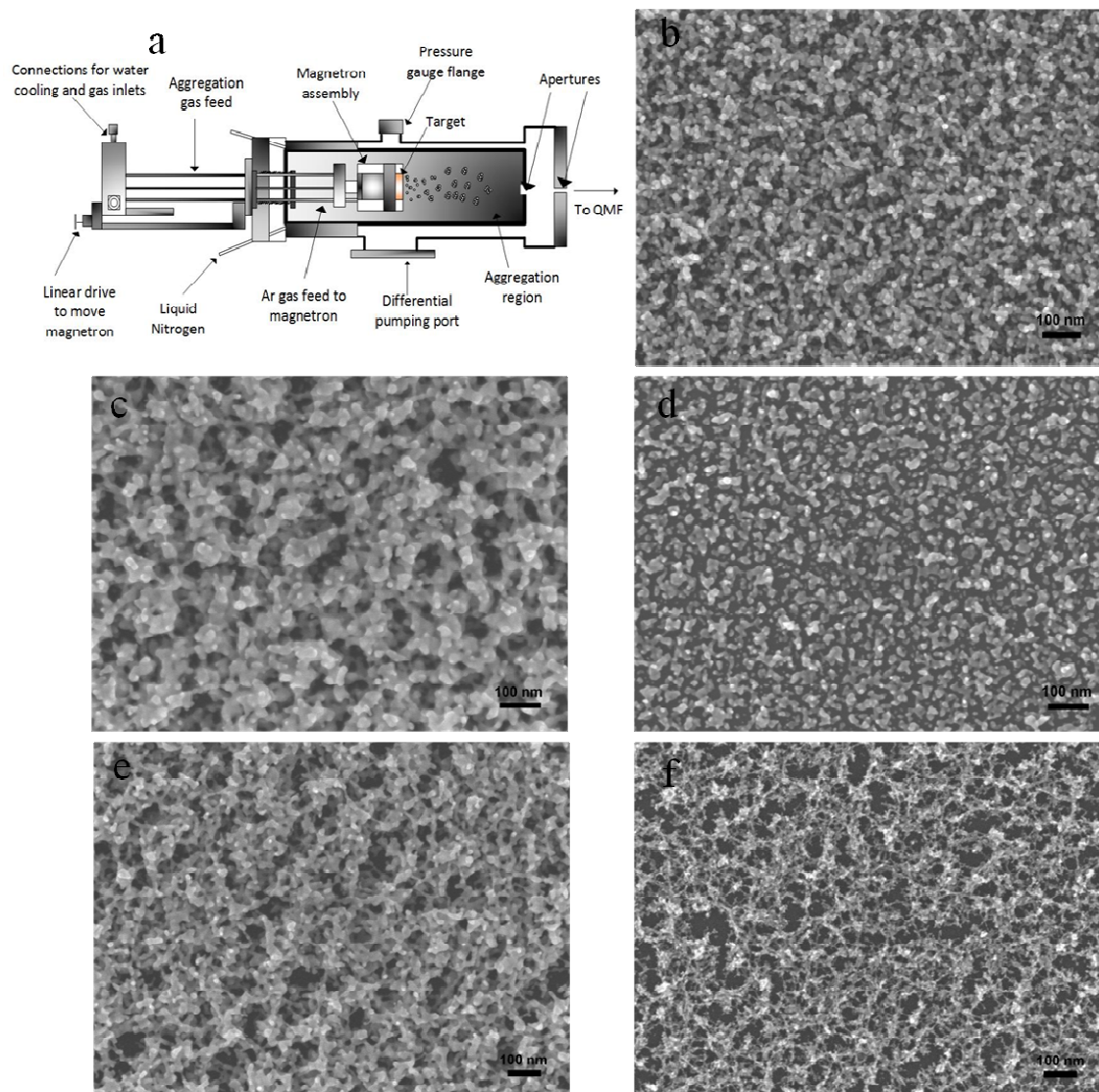


Figure 1 (a) Schematic diagram of the nanocluster source.^[41,49] (b) FE-SEM image of the Au SERS substrate fabricated with QMF on with the selected nanocluster size is 10 nm, the flow rate of Ar is 100 sccm and He is 30 sccm, deposition time is 90 s. FE-SEM images of the Au SERS substrate fabricated with QMF off, the flow rate of Ar is 100 sccm and He is 30 sccm, deposition time is (c) 90 s, (d) 30 s. FE-SEM images of the Au SERS substrate fabricated with QMF off, the flow rate of Ar is 100 sccm and He is 0 sccm, deposition time is (e) 90 s, (f) 30 s. The sputtering power and aggregation length were all set at 115 W and 50 mm, respectively for the above (b) ~ (f).

3.2 SERS homogeneity

To explore the homogeneity of the above three kinds of SERS substrates (the deposition time are all 90 s), 10 μL of 10^{-4} M of R6G solution was dripped on these SERS substrates, and SERS spectra were acquired from 5 different spots within each SERS substrate, respectively. The five positions on each SERS substrate were randomly selected but roughly equally spaced in diagonal direction of substrate. To minimize the influence of “edge effects”,

the SERS spectra were not acquired from the edge positions of each SERS substrate (R6G is a dye, a deeper color can be seen on the edge of each substrate by the optical microscopy attached to the Raman Instrument). From Figure 2, the SERS spectra of R6G obtained from five different locations consist with each other very well in Raman shifts as well as relative intensity (Figure 2a, 2b, 2c). Figure 2d gives a more clear clarification. For the vibration mode at 771 cm^{-1} , the relative standard deviations of the peak intensity were 7.9%, 7.2%, and 9.5% for Figure 2a, 2b, and 2c, respectively. The good homogeneity demonstrates the reliability of these SERS substrates fabricated by this versatile nanocluster fabrication technique, and makes these substrates good candidates for detecting sodium cyclamate.

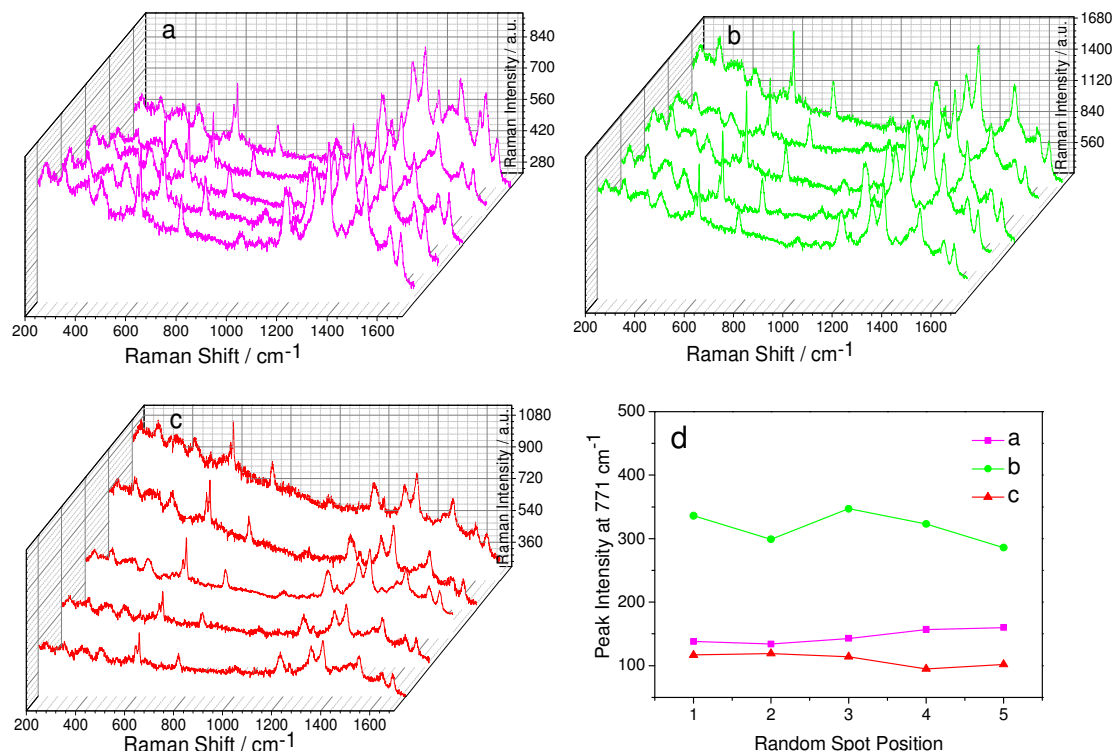


Figure 2 SERS spectra of 10^{-4} M of R6G measured at 5 random spots on the SERS substrate composed of (a) Au nanoparticles; (b) short Au NWs, with small Au nanoparticles filled in the nanogaps (deposition time is 90 s); (c) long Au NWs (deposition time is 90 s). Excitation wavelength: 785 nm; laser power: 0.8 mW; the collected time is 15 s exposure time and three times accumulation for each spectrum. (d) Plots of the peak intensity of R6G at 771 cm^{-1} from 5 random spots on the three SERS substrates.

3.3 EF calculation

R6G is employed as the probe molecule to calculate the EFs of the above three kinds of Au SERS substrates (the deposition time are all 90 s). A 10^{-2} M of R6G solution is employed as the bulk solution, and $10\text{ }\mu\text{L}$ of 10^{-4} M of R6G solution is dripped onto these three SERS substrates, respectively.

$$EF = \frac{I_{surf}}{I_{bulk}} \times \frac{N_{bulk}}{N_{surf}}$$

where I_{surf} and I_{bulk} are the Raman intensities of R6G molecules adsorbed on Au SERS substrate and from a 10^{-2} M of R6G solution, respectively. N_{surf} and N_{bulk} are the

corresponding number of R6G molecules on the Au SERS substrate and in the bulk solution effectively illuminated by the laser beam, respectively.

$$N_{bulk} = Ahc_{bulk}N_A$$

where A is the area of the laser focal spot, c_{bulk} is the concentration of R6G bulk solution, here $c_{bulk} = 10^{-2}$ M, N_A is the Avogadro constant, h is the confocal depth of the laser, here h is 13 μm .^[40]

Provided that R6G molecules were in monolayer adsorption on the Au SERS substrate:

$$N_{surf} = \frac{c_{surf}vN_A A}{\pi r^2}$$

where c_{surf} is the concentration of R6G solution for SERS, here $c_{surf} = 10^{-4}$ M, v is the volume of R6G solution used for SERS detection, here $v = 10$ μL , r is the radius of 10 μL of R6G solution formed on the Au SERS substrate, here $r = 3.5$ mm.

Figure 3a, 3b are the normal Raman spectrum of 10^{-2} M R6G solution and SERS spectrum of 10^{-4} M R6G solution acquired from SERS substrate composed of Au nanoparticles, respectively. The integrated intensities of the bands for I_{bulk} (1513 cm^{-1}) and I_{surf} (1508 cm^{-1}) are 476 and 14494 cps, respectively. Considering the different power of incident laser and the different number of molecules in unit volume,^[40] $I_{surf}/I_{bulk} = 14494 \times 10^4 / 476$.

Finally, the EF of this Au SERS substrate composed of Au nanoparticles (Figure 1b) can be calculated to be 1.52×10^6 .

The integrated intensity of the band for I_{surf} (1512 cm^{-1}) and I_{surf} (1511 cm^{-1}) in Figure 3c, 3d are 20602 and 11969 cps, respectively. Similarly, the EF of the SERS substrate composed of the short Au NWs, with small Au nanoparticles filled in the nanogaps (Figure 1c) can be calculated to be 2.16×10^6 , and the EF of the SERS substrate composed of long Au NWs (Figure 1e) can be calculated to be 1.26×10^6 . Each SERS spectrum in Figure 3b, 3c, and 3d is an average result of the five detections in Figure 2a, 2b, and 2c, respectively.

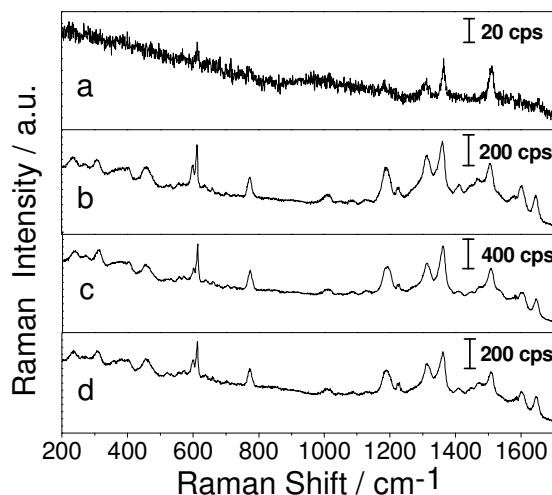


Figure 3 (a) Normal Raman spectrum of 10^{-2} M R6G solution. Laser power: 80 mW. SERS spectrum of 10^{-4} M of R6G solution acquired from the SERS substrate composed of (b) Au nanoparticles; (c) short Au NWs, with small Au nanoparticles filled in the nanogaps (deposition time is 90 s); (d) long Au NWs (deposition time is 90 s). Laser power: 0.8 mW.

Table 1 gives a brief summary about the SERS substrate preparation variables and EFs of the above three typical Au SERS substrates (deposition time is 90 s).

Table 1 Fabrication parameters and EFs of the three typical Au SERS substrates

SERS substrate	QMF	Sputtering power / W	Flow rate of Ar / sccm	Flow rate of He / sccm	Aggregation length / mm	EF
Au nanoparticles (NPs)	on	115	100	30	50	1.52×10^6
Au NWs with small Au NPs filled in the nanogaps	off		100	30		2.16×10^6
long intertwined Au NWs	off		100	0		1.26×10^6

3.4 Enhancement mechanism for the above three kinds of SERS substrates

According to the results in Figure 3, the SERS substrate which is composed of the short Au NWs, with small Au nanoparticles filled in the nanogaps has the highest EF; next is the SERS substrate composed of Au nanoparticles; and the SERS substrate with the constitution of long Au NWs has the relative lowest EF. The EFs of these three substrates are close but still with small differences, and this may result from the intrinsically different nanostructures. When the short Au NWs pile up together, naturally lots of nanogaps will be formed. At the same time, a large amount of small Au nanoparticles filled in these nanogaps shorten the interparticle distance, which creates more hot spots and is beneficial for the SERS enhancement. Similar result can be found in Qian's paper, which demonstrated that nanoporous gold film decorated by gold nanoparticles exhibits 2.9×10^7 augments in comparison with pure nanoporous gold film without any nanoparticle conjugations.^[52] The substrate composed of Au nanoparticles is also ideal for the SERS enhancement. But the Au nanoparticles are not closely-packed enough to make as many hot spots as the small Au nanoparticles filled in the nanogaps does. So the EF of this substrate composed of Au nanoparticles decreases slightly. As for the SERS substrate composed of interlaced long Au NWs, the longer NWs are, the less closely NWs pile up, and the larger the interparticle spacing will tend to be. So in this model, the interparticle distance is enlarged, and the number of hot spots reduces. Therefore, the EF of SERS substrate composed of long Au NWs is the lowest.

3.5 Long-term stability

Furthermore, the long-term stability of three Au SERS substrates (the deposition time are all 90 s) was also investigated. In this work, these three Au SERS substrates were kept in commercial aluminum foil separately in the dark at room temperature over a period of 110 days, then they were took out with care for the stability measurement. R6G was selected as the probe molecules. Each SERS spectrum in Figure 4 is an average result of five detections within the substrate. The five detections were also randomly selected but roughly equally spaced in diagonal direction of substrate. Similarly, the SERS spectra were not acquired from the edge region of each SERS substrate to minimize the influence of "edge effects". After 110

days, the enhancement of SERS substrates composed of Au nanoparticles (Figure 4a), short Au NWs with small Au nanoparticles filled in the nanogaps (Figure 4b), and long Au NWs (Figure 4c) are reduced by 38.9%, 43.8%, and 37.7%, respectively (average results of the vibration mode at 771 cm^{-1} and 1189 cm^{-1}), compared to the SERS spectra obtained from freshly prepared substrates (Figure 3b, 3c, 3d), which demonstrate the long-term stability of three Au SERS substrates. The inactive property of Au, together with the appropriate storage manner keeping Au SERS substrates from contamination are two mainly reasons for the long-term stability.

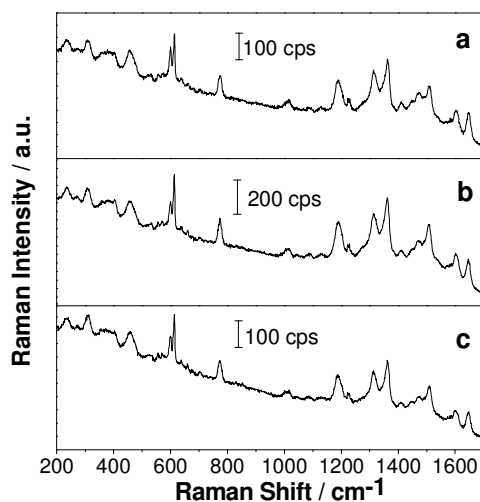


Figure 4 SERS spectrum of 10^{-4} M of R6G solution acquired from (a) Au nanoparticles; (b) short Au NWs, with small Au nanoparticles filled in the nanogaps (deposition time is 90 s); (c) long Au NWs (deposition time is 90 s) after they were saved in commercial aluminum foil for 110 days in the dark at room temperature. Laser power: 0.8 mW.

3.6 SERS detection of sodium cyclamate

Then, among the above three kinds of SERS substrates, the one owns the highest EF was selected and successfully acquired the SERS spectrum of 0.1 M of sodium cyclamate (Figure 5a). The vibrational information of the sodium cyclamate is clearly provided in Figure 5a, and can be used as the reference when identifying illegal addition of this chemical. Compared to the substrates we fabricated in the previous work by the chemical method,^[40] the SERS substrate produced in this work by the physical method has an obvious advantage, that is, it does not need to subtract the substrate interference because there is no contaminant from the reagents, which makes the technique in this work an ideal approach for fabricating SERS-active substrates for fast detection. Figure 5b is also the SERS spectrum of 0.1 M of sodium cyclamate, but acquired from the plain and dense gold film substrate prepared by a common physical fabrication technique (sputter coating). Compared these two spectra in Figure 5, the major Raman shifts consist with each other very well, while the plain and dense gold film substrate gives a relative low SERS enhancement, about 10 times lower than the SERS intensity acquired from the substrate composed of short Au NWs, with small Au nanoparticles filled in the nanogaps.

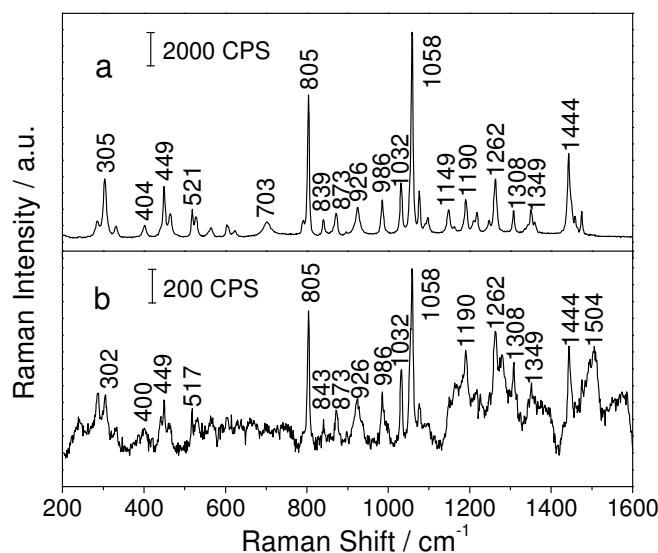


Figure 5 The SERS spectrum of 0.1 M of sodium cyclamate acquired from (a) the substrate composed of short Au NWs, with small Au nanoparticles filled in the nanogaps; (b) the plain and dense gold film substrate prepared by the sputter coating technique (40 mA, 150 s). Excitation wavelength: 785 nm; laser power: 8 mW. The collected time is 15 s exposure time and 3 scans.

3.7 Relationship between SERS intensity and sodium cyclamate concentration

Next, to evaluate the sensitivity of this food additive with the SERS substrate, a series of SERS spectra of sodium cyclamate under different concentrations were detected. 10 μL of each concentration (10^{-9} M~ 10^{-1} M) was dripped on the SERS substrate owns the highest EF, respectively, and waited until they dried under ambient conditions, then SERS spectra were acquired (Figure 6a). In Figure 6a, the SERS spectra of sodium cyclamate were well obtained, and the spectra intensity decreases along with the concentration decreasing.

Figure 6b is the correlation between the SERS intensity and the sodium cyclamate concentration. The SERS peak intensity of sodium cyclamate at 804 cm^{-1} was set as y axis, and the sodium cyclamate concentration was set as x axis. Same as the result in our previous paper^[37], there exists two linear regions in the whole concentration range. When the sodium cyclamate concentration is in the range of 10^{-3} ~ 10^{-1} M, the linear regression equation is $y=2407.8\log(x) + 10776.8$, and the correlation coefficient is 0.993 (n=3). When the sodium cyclamate concentration is in the range of 10^{-9} ~ 10^{-3} M, the linear regression equation is $y=609.2\log(x) + 5373.7$, and the correlation coefficient is 0.995 (n=7). The detection limit of sodium cyclamate can be calculated to be 1.6×10^{-9} M according to the signal / noise ratio of three.

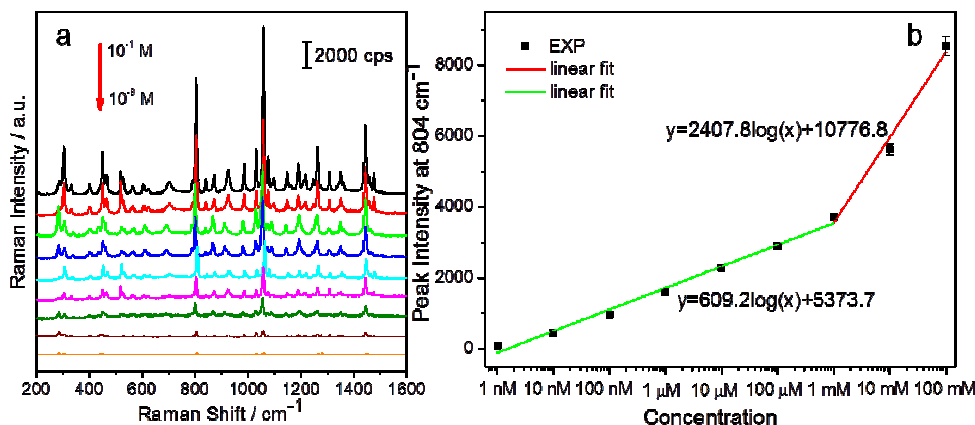


Figure 6 (a) Concentration-dependent SERS spectra for sodium cyclamate detection (10^{-1} M– 10^{-9} M), which were obtained from the SERS substrate composed of short Au NWs, with small Au nanoparticles filled in the nanogaps. Excitation wavelength: 785 nm; laser power: 8 mW. (b) Piecewise linearity plots of SERS intensity of sodium cyclamate at 804 cm^{-1} vs. sodium cyclamate concentration.

4. Conclusions

In this work, we introduced a versatile nanoclusters fabrication technique to prepare Au SERS-active substrates, which allows the pre-selection of the nanocluster size. Three typical SERS substrates, which composed of Au nanoparticles, short Au NWs with small Au nanoparticles filled in the nanogaps, and long Au NWs intertwining one another into a self-supporting film, were fabricated respectively by this system under different parameters. These three SERS substrates have good homogeneity, long-term stability, and their EFs are all at the order of 10^6 by using R6G as probe molecules. Then the SERS spectrum of sodium cyclamate, one food additive, was successfully acquired from the SERS substrate with the highest EF, which composed of small Au nanoparticles distributed around short Au NWs, and its SERS intensity is 10 times higher than the SERS intensity obtained from the plain and dense Au film substrate prepared by a common physical fabrication technique. Finally, the correlation between SERS intensity and sodium cyclamate concentration was given, and a set of piecewise-linear equations were also provided with a detection limit down to 1.6×10^{-9} M. This technique is time-efficient, easy to prepare large-area SERS substrates with tunable nanostructures, and can also produce chemical clean SERS substrates, which suggest this versatile nanofabrication technique is promising for reliable SERS substrates fabrication, and the potential application of the produced SERS substrates in chemical molecules detection.

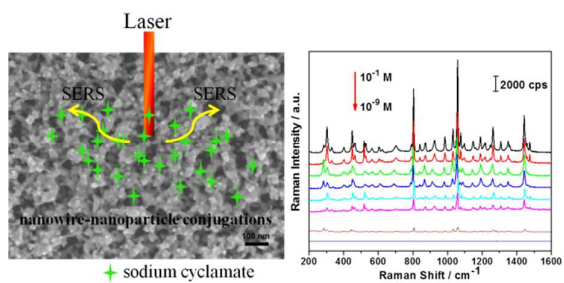
Acknowledgments

We thank Ronald Gary, Casey Hall-Wheeler, and Shirley Shen from UNLV for assistance with ultrapure water. This work was supported by the National Natural Science Foundation of China (No. 50871028) and the Fundamental Research Funds for the Central Universities (No. N110610001). G. W. Qin appreciates Program for New Century Excellent Talents in University (No. NCET-10-0272). J. Chen appreciates the assistance from China Scholarship Council (CSC), and Northeastern University excellent doctoral dissertation breeding program, China.

References

- [1] Golightly, R. S.; Doering, W. E.; Natan, M. J. *ACS Nano* 2009, 3, 2859-2869.
- [2] Camden, J. P.; Dieringer, J. A.; Zhao, J.; Van Duyne, R. P. *Accounts Chem. Res.* 2008, 41, 1653-1661.
- [3] Le Ru, E. C.; Etchegoin, P. G. *Principles of Surface Enhanced Raman Spectroscopy and Related Plasmonic Effects*; Elsevier: Amsterdam, Netherlands, 2009.
- [4] Nie, S. M.; Emory, S. R. *Science* 1997, 275, 1102-1106.
- [5] Kneipp, K.; Wang, Y.; Kneipp, H.; Perelman, L. T.; Itzkan, I.; Dasari, R.; Feld, M. S. *Phys. Rev. Lett.* 1997, 78, 1667-1670.
- [6] Qian, C.; Ni, C.; Yu W. X.; Wu, W. G.; Mao, H. Y.; Wang, Y. F.; Xu, J. *Small* 2011, 7, 1801-1806.
- [7] Barhoumi, A.; Halas, N. J. *J. Am. Chem. Soc.* 2010, 132, 12792-12793.
- [8] Lal, S.; Grady, N. K.; Kundu, J.; Levin, C. S.; Lassiter, J. B.; Halas, N. J. *Chem. Soc. Rev.* 2008, 37, 898-911.
- [9] Mayer, K. M.; Hafner, J. H. *Chem. Rev.* 2011, 111, 3828-3857.
- [10] Lee, W.; Lee, S. Y.; Briber, R. M.; Rabin, O. *Adv. Funct. Mater.* 2011, 21, 3424-3429.
- [11] Vitol, E. A.; Orynbayeva, Z.; Bouchard, M. J.; Azizkhan-Clifford, J.; Friedman, G.; Gogotsi, Y. *ACS Nano* 2009, 3, 3529-3536.
- [12] Matschulat, A.; Drescher, D.; Kneipp, J. *ACS Nano* 2010, 4, 3259-3269.
- [13] Pallaoro, A.; Braun, G. B.; Moskovits, M. *Proc. Natl. Acad. Sci. USA* 2011, 108, 16559-16564.
- [14] Theiss, J.; Pavaskar, P.; Echternach, P. M.; Muller, R. E.; Cronin, S. B. *Nano Lett.* 2010, 10, 2749-2754.
- [15] Qian, X. M.; Peng, X. H.; Ansari, D. O.; Yin-Goen, Q.; Chen, G. Z.; Shin, D. M.; Yang, L.; Young, A. N.; Wang, M. D.; Nie, S. M. *Nat. Biotechnol.* 2008, 26, 83-90.
- [16] Wang, G. F.; Lipert, R. J.; Jain, M.; Kaur, S.; Chakraborty, S.; Torres, M. P.; Batra, S. K.; Brand, R. E.; Porter, M. D. *Anal. Chem.* 2011, 83, 2554-2561.
- [17] Halvorson, R. A.; Vikesland, P. J. *Environ. Sci. Technol.* 2010, 44, 7749-7755.
- [18] Kong, K. V.; Lam, Z. Y.; Lau, W. K. O.; Leong, W. K.; Oivo, M. *J. Am. Chem. Soc.* 2013, 135, 18028-18031.
- [19] Qian, X. M.; Zhou, X.; Nie, S. M. *J. Am. Chem. Soc.* 2008, 130, 14934-14935.
- [20] Liu, S. P.; Chen, N.; Li, L. X.; Pang, F. F.; Chen, Z. Y.; Wang, T. Y. *Opt. Mater.* 2013, 35, 690-692.
- [21] Kundu, S. J. *J. Mater. Chem. C* 2013, 1, 831-842.
- [22] Kundu, S.; Jayachandran, M. *RSC Advances* 2013, 3, 16486-16498.
- [23] Hong, G. S.; Li, C.; Qi, L. M. *Adv. Funct. Mater.* 2010, 20, 3774-3783.
- [24] Chang, S.; Combs, Z. A.; Gupta, M. K.; Davis, R.; Tsukruk, V. V. *ACS Appl. Mater. Inter.* 2010, 2, 3333-3339.
- [25] Bechelany, M.; Brodard, P.; Elias, J.; Brioude, A.; Michler, J.; Philippe, L. *Langmuir* 2010, 26, 14364-14371.
- [26] Ye, X. Z.; Qi, L. M. *Nano Today* 2011, 6, 608-631.
- [27] Paczesny, J.; Kaminska, A.; Adamkiewicz, W.; Winkler, K.; Sozanski, K.; Wadowska, M.; Dziecielewski, I.; Holyst, R. *Chem. Mater.* 2012, 24, 3667-3673.

- [28] Chen, M. S.; Phang, I. Y.; Lee, M. R.; Yang, J. K. W.; Ling, X. Y. *Langmuir* 2013, 29, 7061-7069.
- [29] Gunawidjaja, R.; Kharlampieva, E.; Choi, I.; Tsukruk, V. V. *Small* 2009, 5, 2460-2466.
- [30] Lee, S. J.; Baik, J. M.; Moskovits, M. *Nano Lett.* 2008, 8, 3244-3247.
- [31] Guo, S. J.; Dong, S. J.; Wang, E. K. *Cryst. Growth Des.* 2009, 9, 372-377.
- [32] Wang, H.; Levin, C. S.; Halas, N. J. *J. Am. Chem. Soc.* 2005, 127, 14992-14993.
- [33] Tao, A.; Kim, F.; Hess, C.; Goldberger, J.; He, R. R.; Sun, Y. G.; Xia, Y. N.; Yang, P. D. *Nano Lett.* 2003, 3, 1229-1233.
- [34] Chen, C. F.; Hao, J. M.; Zhu, L. Y.; Yao, Y. Q.; Meng, X. G.; Weimer, W.; Wang, Q. W. *J. Mater. Chem. A* 2013, 1, 13496-13501.
- [35] Freer, E. M.; Grachev, O.; Duan, X. F.; Martin, S.; Stumbo, D. P. *Nat. Nanotechnol.* 2010, 5, 525-530.
- [36] Zhang, X. Y.; Hu, A. M.; Zhang, T.; Lei, W.; Xue, X. J.; Zhou, Y. H.; Duley, W. W. *ACS nano* 2011, 5, 9082-9092.
- [37] Chen, J.; Qin, G. W.; Wang, J. S.; Yu, J. Y.; Shen, B.; Li, S.; Ren, Y. P.; Zuo, L.; Shen, W.; Das, B. *Biosens. Bioelectron.* 2013, 44, 191-197.
- [38] Smith, W. E. *Chem. Soc. Rev.* 2008, 37, 955-964.
- [39] Huang, J. Y.; Zong, C.; Xu, L. J.; Cui, Y.; Ren, B. *Chem. Commun.* 2011, 47, 5738-5740.
- [40] Chen, J.; Shen, B.; Qin, G. W.; Hu, X. W.; Qian, L. H.; Wang, Z. W.; Li, S.; Ren, Y. P.; Zuo, L. *J. Phys. Chem. C* 2012, 116, 3320-3328.
- [41] Banerjee, A.; Das, B. *Rev. Sci. Instrum.* 2008, 79, 033910.
- [42] Culha, M.; Cullum, B.; Lavrik, N.; Klutse, C.K. *J. Nanotechnol.* 2012, 971380.
- [43] Weihrauch, M. R.; Diehl, V. *Ann. Oncol.* 2004, 15, 1460-1465.
- [44] Gaunt, I. F.; Sharratt, M.; Grasso, P.; Lansdown, A. B. G.; Gangolli, S. D. *Food Cosmet. Toxicol.* 1974, 12, 609-624.
- [45] James, R. W.; Heywood, R.; Crook, D. *Food Cosmet. Toxicol.* 1981, 19, 291-296.
- [46] Roberts, A.; Renwick, A. G. *Toxicol. Appl. Pharmacol.* 1989, 98, 230-242.
- [47] Roberts, A.; Renwick, A. G.; Ford, G.; Creasy, D. M.; Gaunt, I. *Toxicol. Appl. Pharmacol.* 1989, 98, 216-229.
- [48] Armenta, S.; Garrigues, S.; de la Guardia, M. *Anal. Chim. Acta.* 2004, 521, 149-155.
- [49] <http://www.oaresearch.co.uk>
- [50] Das, B.; Banerjee, A. *Nanotechnology* 2007, 18, 445202.
- [51] Banerjee, A. N.; Krishna, R.; Das, B. *Appl. Phys. A* 2008, 90, 299-303.
- [52] Qian, L. H.; Das, B.; Li, Y.; Yang, Z. L. *J. Mater. Chem.* 2010, 20, 6891-6895.



Three tunable Au SERS nanostructures (nanoparticles, nanowire-nanoparticle conjugations, nanofilm) were fabricated, and used for sodium cyclamate detection.